

Electronic Supporting Information

Reversible Luminescent "Off-On" Regulation Based on Tunable Photodimerization via Crystal-to-Cocrystal Transformation

Yufei Wang,^{ab} Hongxing Shang,^{ab} Bao Li^b and Shimei Jiang^{*ab}

^aEngineering Research Center of Organic and Polymer Optoelectronic Materials,
Ministry of Education, College of Chemistry, Jilin University, 2699 Qianjin Street,
Changchun 130012, P. R. China

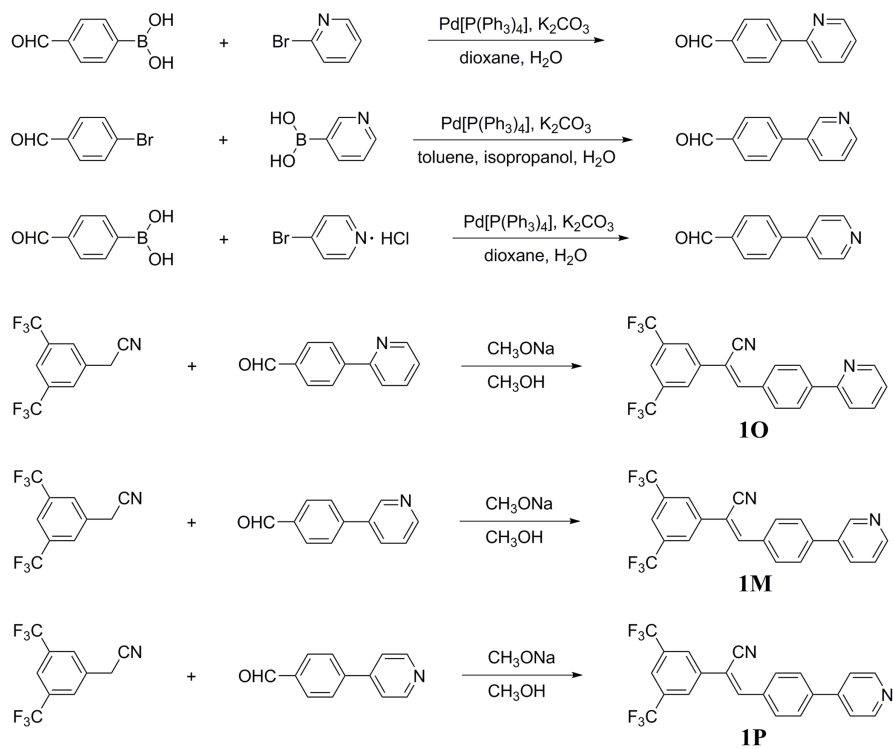
^bState Key Laboratory of Supramolecular Structure and Materials, College of
Chemistry, Jilin University, 2699 Qianjin Street, Changchun 130012, P. R. China

E-mail: smjiang@jlu.edu.cn

Contents

1. Synthesis and characterization of compounds.....S2
2. Photophysical properties and crystal data.....S9
3. Photodimerization reaction.....S12
4. Characterization of cocrystals.....S16

1. Synthesis and characterization of compounds



Scheme S1 Synthetic routes of 1O, 1M and 1P.

Synthesis of 4-(pyridin-2-yl)benzaldehyde

(4-formylphenyl)boronic acid (1.74 g, 11.6 mmol) and K_2CO_3 (4.26 g, 30.8 mmol) were dispersed in the mixture solvent of 60.0 mL of 1,4-dioxane and 15.0 mL of water. The solution was stirred at room temperature and bubbled with nitrogen for 30 min. Then 2-bromopyridine (735 μ L, 1.22 g, 7.71 mmol) and $Pd(PPh_3)_4$ (0.45 g, 0.39 mmol) were added. The mixture was heated to reflux. After 9 hours, the reaction mixture was cooled to room temperature and solvent was removed on a rotary evaporator. The residue was poured into saturated salt water and extracted with ethyl acetate. The organic layer was dried over $MgSO_4$. After filtration and solvent evaporation, the crude product was purified by silica-gel chromatography using ethyl acetate/hexane mixture (1:2, v/v) as eluent to obtain 4-(pyridin-2-yl)benzaldehyde (1.20 g, yield 81%).

1H -NMR (500 MHz, $CDCl_3$) δ /ppm = 10.09 (s, 1H), 8.75 (d, J = 4.7 Hz, 1H), 8.18 (d, J = 8.1 Hz, 2H), 8.00 (d, J = 8.1 Hz, 2H), 7.82 (d, J = 3.7 Hz, 2H), 7.38-7.28 (m, 1H).

Synthesis of 4-(pyridin-3-yl)benzaldehyde

4-bromobenzaldehyde (1.50 g, 8.10 mmol), pyridin-3-ylboronic acid (1.20 g, 9.76 mmol) and K_2CO_3 (4.26 g, 30.8 mmol) were dispersed in the mixture solvent of 40.0 mL of toluene, 15.0 mL of isopropanol and 15.0 mL of water. The solution was stirred at room temperature and bubbled with nitrogen for 30 min. Then $Pd(PPh_3)_4$ (0.45 g, 0.39 mmol) was added. The mixture was heated to reflux. After 9 hours, the reaction mixture was cooled to room temperature and solvent was removed on a rotary evaporator. The residue was poured into saturated salt water and extracted with ethyl acetate. The organic layer was dried over $MgSO_4$. After filtration and solvent evaporation, the crude product was purified by silica-gel chromatography using CH_2Cl_2 /hexane mixture (2:1, v/v) as eluent to obtain 4-(pyridin-3-yl)benzaldehyde (0.83 g, yield 56%).

1H -NMR (500 MHz, $CDCl_3$) δ /ppm = 10.09 (s, 1H), 8.91 (d, J = 1.7 Hz, 1H), 8.67 (d, J = 4.5 Hz, 1H), 8.01 (d, J = 8.1 Hz, 2H), 7.94 (d, J = 7.9 Hz, 1H), 7.77 (d, J = 8.1 Hz, 2H), 7.43 (dd, J = 7.8, 4.8 Hz, 1H).

Synthesis of 4-(pyridin-4-yl)benzaldehyde

(4-formylphenyl)boronic acid (1.50 g, 7.71 mmol), 4-bromopyridine hydrochloride (1.74 g, 11.6 mmol) and K_2CO_3 (4.26 g, 30.8 mmol) were dispersed in the mixture solvent of 60.0 mL of 1,4-dioxane and 15.0 mL of water. The solution was stirred at room temperature and bubbled with nitrogen for 30 min. Then $Pd(PPh_3)_4$ (0.45 g, 0.39 mmol) was added. The mixture was heated to reflux. After 9 hours, the reaction mixture was cooled to room temperature and solvent was removed on a rotary evaporator. The residue was poured into saturated salt water and extracted with CH_2Cl_2 . The organic layer was dried over $MgSO_4$. After filtration and solvent evaporation, the crude product was purified by silica-gel chromatography using ethyl acetate/hexane mixture (2:1, v/v) as eluent to obtain 4-(pyridin-4-yl)benzaldehyde (1.36 g, yield 92%).

1H -NMR (500 MHz, $CDCl_3$) δ/ppm = 10.10 (s, 1H), 8.73 (dd, J = 4.6, 1.5 Hz, 2H), 8.01 (d, J = 8.2 Hz, 2H), 7.81 (d, J = 8.2 Hz, 2H), 7.55 (dd, J = 4.6, 1.5 Hz, 2H).

Synthesis of 1O

(Z)-2-(3,5-bis(trifluoromethyl)phenyl)-3-(4-(pyridin-2-yl)-phenyl)acrylonitrile

2-(3,5-bis(trifluoromethyl)phenyl)acetonitrile (0.55 mL, 0.76 g, 3.0 mmol) and 4-(pyridin-2-yl)benzaldehyde (0.55 g, 3.0 mmol) were dissolved in 15.0 mL of 20 mM CH_3ONa/CH_3OH . The mixture was stirred at room temperature for two days. After that, the precipitate was filtered and washed several times with methanol and water, respectively. The product was obtained (1.03 g, yield 82%).

1H -NMR (500 MHz, $CDCl_3$) δ/ppm = 8.75 (d, J = 4.7 Hz, 1H), 8.18 (d, J = 8.3 Hz, 2H), 8.13 (s, 2H), 8.08 (d, J = 8.4 Hz, 2H), 7.92 (s, 1H), 7.83 (d, J = 3.8 Hz, 2H), 7.71 (s, 1H), 7.32 (q, J = 4.7 Hz, 1H). ^{13}C -NMR (126 MHz, $CDCl_3$) δ/ppm = 155.89, 150.06, 144.92, 142.40, 137.16, 136.92, 133.20, 132.88 (q, J = 33.80 Hz), 130.36, 127.68, 126.15, 123.12, 123.09 (q, J = 273.58 Hz), 122.83, 120.99, 117.14 and 109.07. Anal. Calc. for $C_{22}H_{12}F_6N_2$: C, 63.16; H, 2.89; N, 6.70. Found: C, 63.73; H, 2.74; N, 6.66. MS: m/z = 418.36.

Synthesis of 1M

(Z)-2-(3,5-bis(trifluoromethyl)phenyl)-3-(4-(pyridin-3-yl)-phenyl)acrylonitrile

2-(3,5-bis(trifluoromethyl)phenyl)acetonitrile (0.55 mL, 0.76 g, 3.0 mmol) and 4-(pyridin-3-yl)benzaldehyde (0.55 g, 3.0 mmol) were dissolved in 15.0 mL of 20 mM CH₃ONa/CH₃OH. The mixture was stirred at room temperature for two days. After that, the precipitate was filtered and washed several times with methanol and water, respectively. The product was obtained (1.13 g, yield 90%).

¹H-NMR (500 MHz, CDCl₃) δ/ppm = 8.91 (d, *J* = 1.8 Hz, 1H), 8.65 (dd, *J* = 4.8, 1.6 Hz, 1H), 8.12 (s, 2H), 8.07 (d, *J* = 8.3 Hz, 2H), 7.98-7.93 (m, 1H), 7.92 (s, 1H), 7.74 (d, *J* = 8.4 Hz, 2H), 7.71 (s, 1H), 7.45-7.36 (m, 1H). ¹³C-NMR (126 MHz, CDCl₃) δ/ppm = 149.47, 148.33, 144.61, 141.08, 136.77, 135.33, 134.51, 132.92 (q, *J* = 33.86 Hz), 132.55, 130.60, 127.90, 126.16, 123.89, 123.06 (q, *J* = 273.52 Hz), 122.93, 117.08 and 109.36. Anal. Calc. for C₂₂H₁₂F₆N₂: C, 63.16; H, 2.89; N, 6.70. Found: C, 63.98; H, 2.66; N, 6.74. MS: *m/z* = 418.36.

Synthesis of 1P

(Z)-2-(3,5-bis(trifluoromethyl)phenyl)-3-(4-(pyridin-4-yl)-phenyl)acrylonitrile

2-(3,5-bis(trifluoromethyl)phenyl)acetonitrile (0.55 mL, 0.76 g, 3.0 mmol) and 4-(pyridin-4-yl)benzaldehyde (0.55 g, 3.0 mmol) were dissolved in 15.0 mL of 20 mM CH₃ONa/CH₃OH. The mixture was stirred at room temperature for two days. After that, the precipitate was filtered and washed several times with methanol and water, respectively. The product was obtained (1.07 g, yield 85%).

¹H-NMR (500 MHz, CDCl₃) δ/ppm = 8.72 (d, *J* = 5.6 Hz, 2H), 8.12 (s, 2H), 8.08 (d, *J* = 8.2 Hz, 2H), 7.92 (s, 1H), 7.79 (d, *J* = 8.3 Hz, 2H), 7.71 (s, 1H), 7.56 (d, *J* = 5.7 Hz, 2H). ¹³C-NMR (126 MHz, CDCl₃) δ/ppm = 150.56, 147.00, 144.41, 141.22, 136.67, 133.45, 132.96 (q, *J* = 33.97 Hz), 130.58, 127.89, 126.22, 123.05, 123.05 (q, *J* = 273.46 Hz), 121.64, 116.98 and 109.86. Anal. Calc. for C₂₂H₁₂F₆N₂: C, 63.16; H, 2.89; N, 6.70. Found: C, 63.76; H, 2.96; N, 6.67. MS: *m/z* = 418.34.

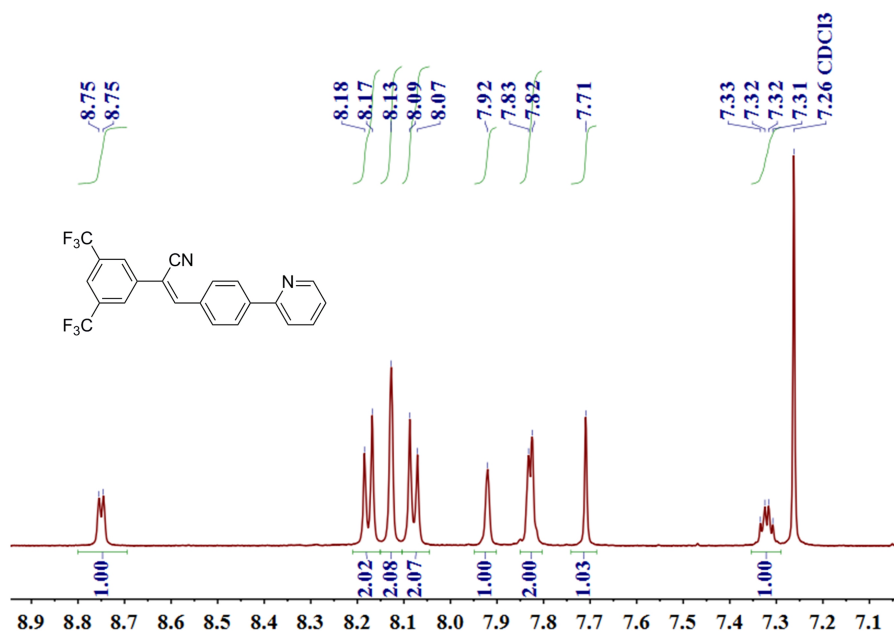


Fig. S1 $^1\text{H-NMR}$ spectrum of 1O (14 mM) in CDCl_3 .

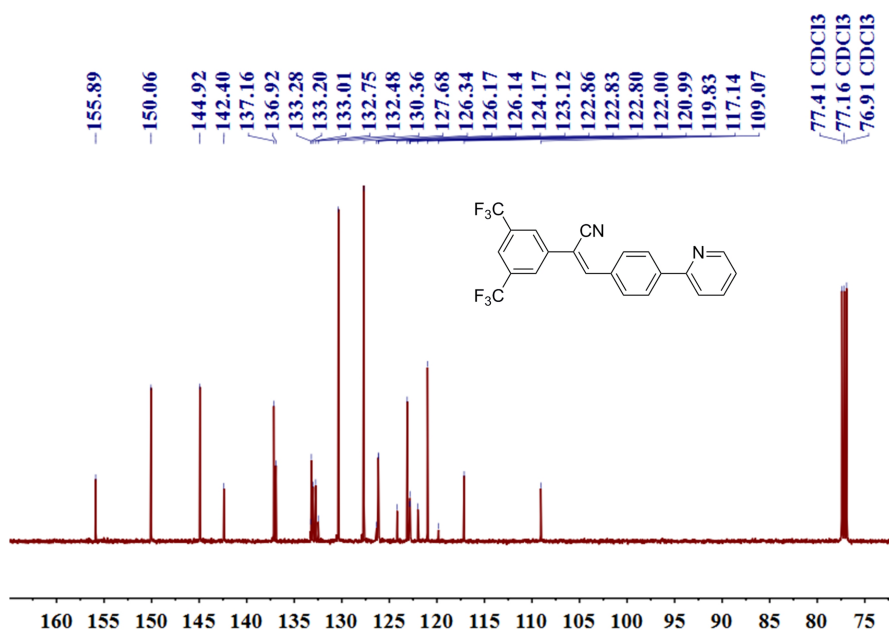


Fig. S2 $^{13}\text{C-NMR}$ spectrum of 1O (98 mM) in CDCl_3 .

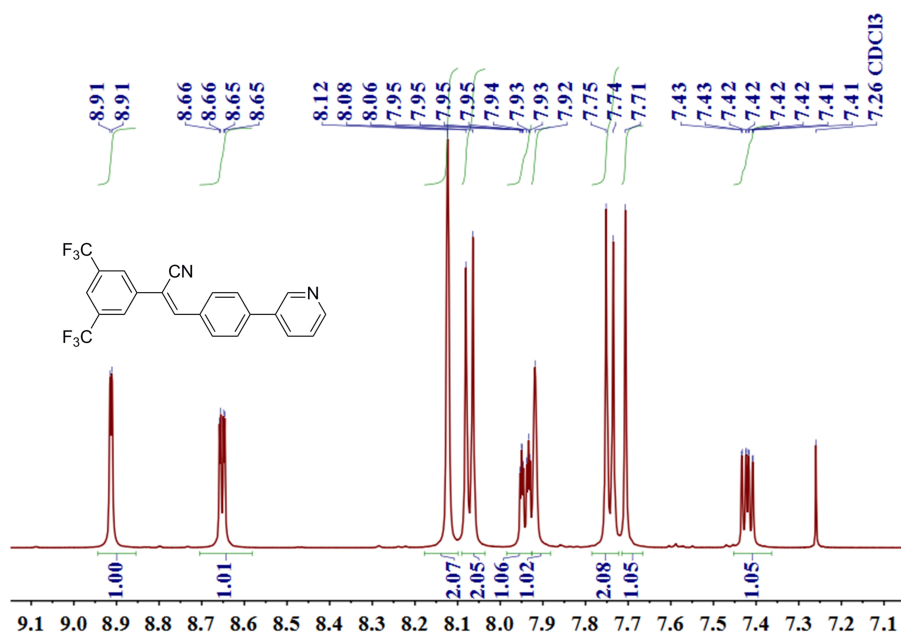


Fig. S3 ¹H-NMR spectrum of 1M (98 mM) in CDCl₃.

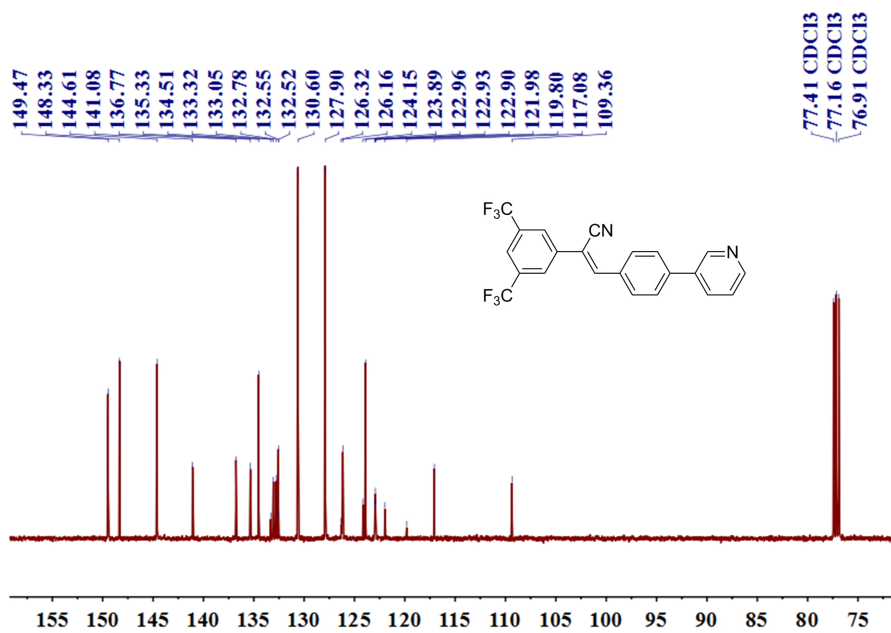


Fig. S4 ¹³C-NMR spectrum of 1M (98 mM) in CDCl₃.

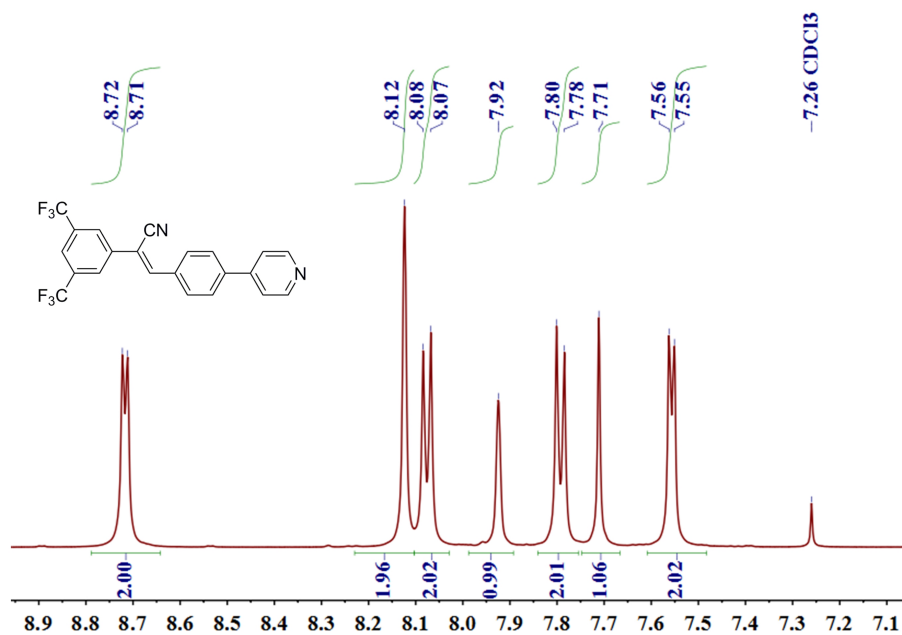


Fig. S5 ¹H-NMR spectrum of 1P (98 mM) in CDCl₃.

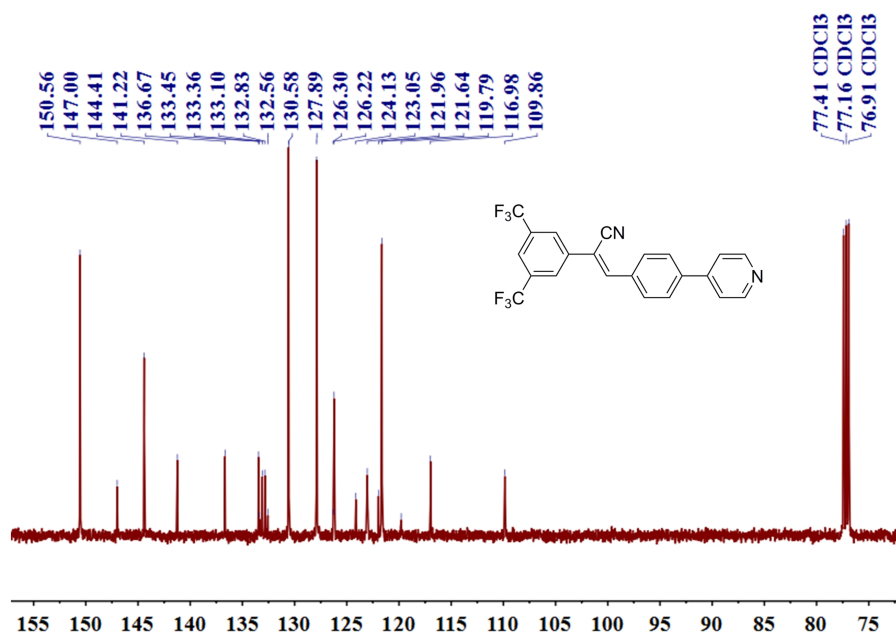


Fig. S6 ¹³C-NMR spectrum of 1P (98 mM) in CDCl₃.

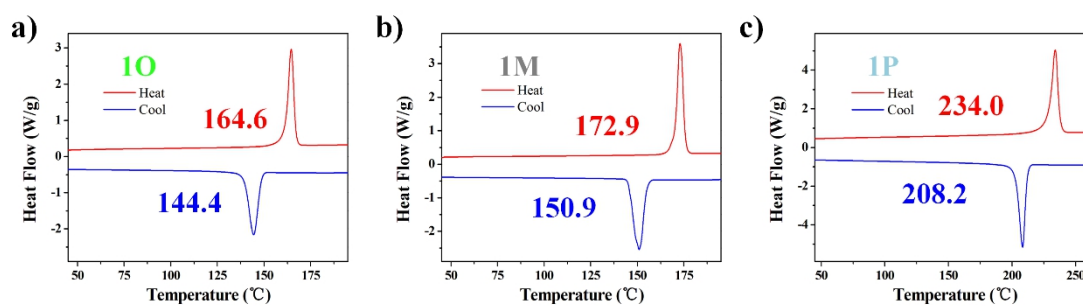


Fig. S7 DSC traces of (a) 1O, (b) 1M and (c) 1P (20 °C min⁻¹ on the second cycle).

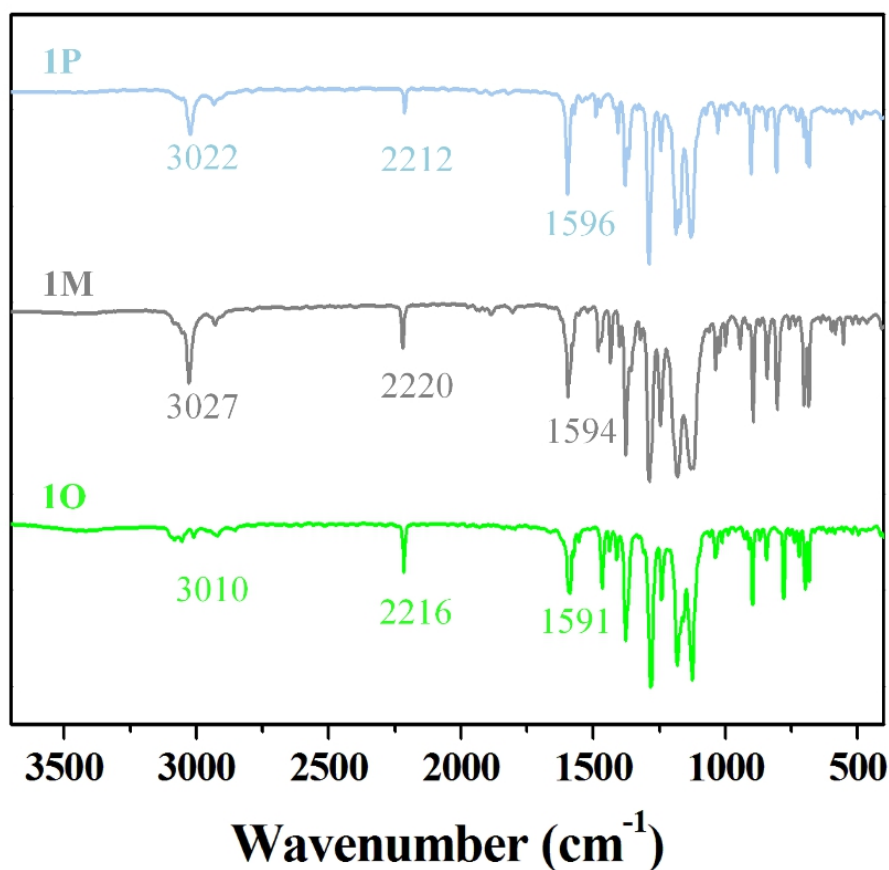


Fig. S8 FT-IR spectra of 1O, 1M and 1P.

2. Photophysical properties and crystal data

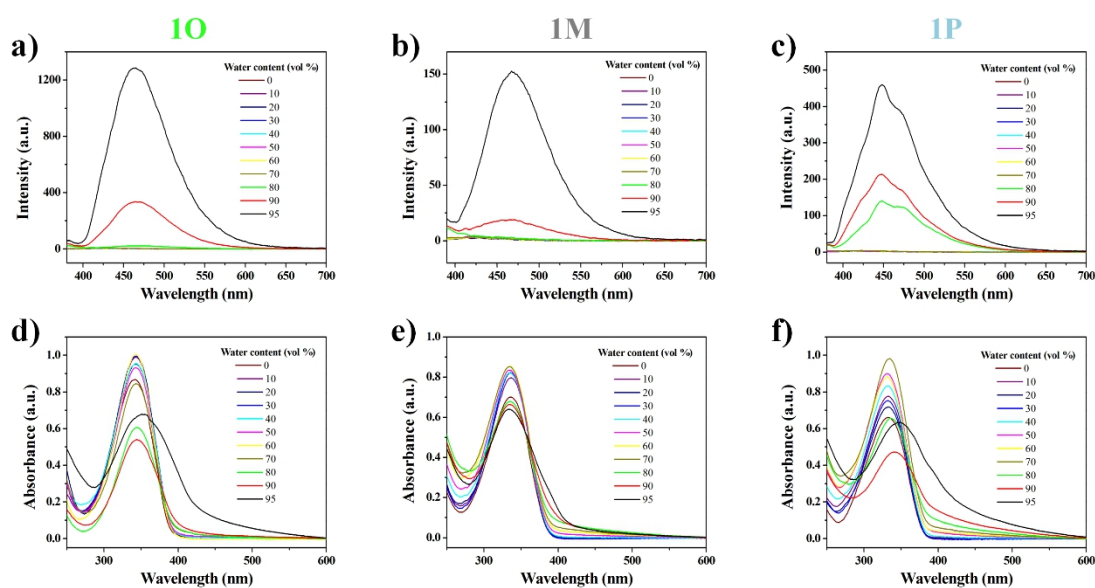


Fig. S9 PL spectra of (a) 1O, (b) 1M and (c) 1P in THF/H₂O mixtures with different water content (λ_{ex} = 370 nm). Accordingly, UV-vis spectra of (d) 1O, (e) 1M and (f) 1P in THF/H₂O mixtures with different water content (20 μ M).

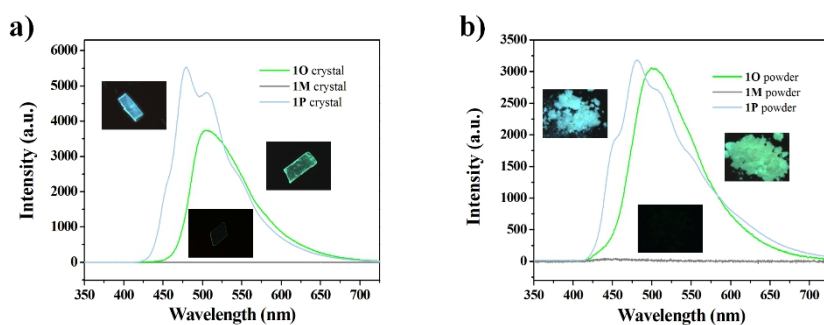


Fig. S10 PL spectra of (a) crystals and (b) powders for 1O, 1M and 1P. The insets show the fluorescent microphotographs of crystals and powders, respectively ($\lambda_{\text{ex}} = 365$ nm).

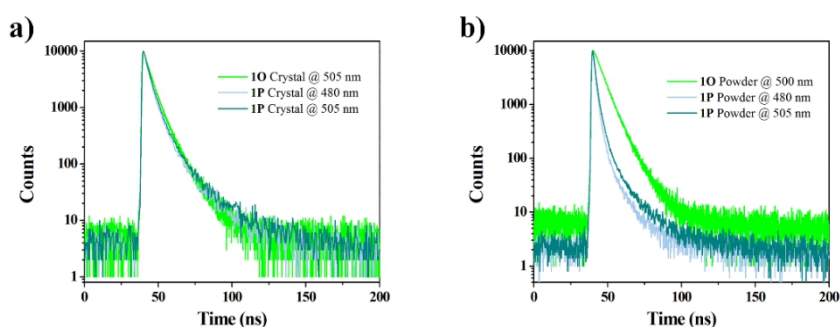


Fig. S11 The lifetimes of 1O and 1P in (a) the crystal states and (b) the powder states ($\lambda_{\text{ex}} = 365$ nm).

Table S1 The photophysical properties of 1O and 1P

Compound	state	PL (nm)	τ (ns)	PLQY	k_r (s^{-1}) ^a	k_{nr} (s^{-1}) ^b
1O	powder	500	6.365	0.36	5.686×10^7	1.003×10^8
	crystal	505	$\tau_1 = 4.93$ (0.82) $\tau_2 = 12.70$ (0.18)	0.29	4.509×10^7	1.129×10^8
1P	powder	480	$\tau_1 = 1.60$ (0.85) $\tau_2 = 7.24$ (0.15)	0.42	1.700×10^8	2.390×10^8
		505	$\tau_1 = 1.91$ (0.83) $\tau_2 = 8.83$ (0.17)		1.349×10^8	1.896×10^8
	crystal	480	$\tau_1 = 3.67$ (0.75) $\tau_2 = 12.73$ (0.25)	0.38	6.427×10^7	1.043×10^8
		505	$\tau_1 = 4.22$ (0.80) $\tau_2 = 15.59$ (0.20)		5.871×10^7	9.531×10^7

^aRadiative transition rate constant: $k_r = \Phi_F / \langle \tau \rangle$.

^bNon-radiative transition rate constant: $k_{\text{nr}} = (1 - \Phi_F) / \langle \tau \rangle$. $\langle \tau \rangle = (A_1 \tau_1^2 + A_2 \tau_2^2) / (A_1 \tau_1 + A_2 \tau_2)$.

Table S2 Crystal data and structure refinements for 1O, 1M and 1P

Compound	1O	1M	1P
Empirical formula	C ₂₂ H ₁₂ F ₆ N ₂	C ₂₂ H ₁₂ F ₆ N ₂	C ₂₂ H ₁₂ F ₆ N ₂
Formula weight/g mol ⁻¹	418.34	418.34	418.34
<i>T</i> /K	293(2)	293(2)	293(2)
λ /Å	0.71073	0.71073	0.71073
Crystal system	Monoclinic	Monoclinic	Triclinic
Space group	<i>P</i> 2/ <i>c</i>	<i>C</i> 2/ <i>c</i>	<i>P</i> -1
Unit cell dimensions/Å	<i>a</i> = 15.858(2) <i>b</i> = 8.8033(12) <i>c</i> = 13.6717(18)	<i>a</i> = 27.4290(13) <i>b</i> = 9.1587(4) <i>c</i> = 15.1392(6)	<i>a</i> = 8.7740(18) <i>b</i> = 9.0110(18) <i>c</i> = 11.624(2)
Unit cell angles/°	α = 90 β = 95.506(6) γ = 90	α = 90 β = 98.565(3) γ = 90	α = 85.74(3) β = 88.18(3) γ = 86.44(3)
Volume/Å ³	1899.8(4)	3760.8(3)	914.4(3)
<i>Z</i>	4	8	2
ρ (calculated)/Mg m ⁻³	1.463	1.478	1.519
Absorption coefficient/mm ⁻¹	0.128	0.129	0.133
<i>F</i> (000)	848	1696	424
Crystal size/mm ³	0.140 × 0.120 × 0.100	0.130 × 0.120 × 0.100	0.13 × 0.12 × 0.10
θ range for data collection/°	2.982 to 27.558	2.656 to 28.308	3.15 to 27.48
Index ranges	-20 ≤ <i>h</i> ≤ 18, -11 ≤ <i>k</i> ≤ 11, -17 ≤ <i>l</i> ≤ 16	-36 ≤ <i>h</i> ≤ 36, -12 ≤ <i>k</i> ≤ 12, -20 ≤ <i>l</i> ≤ 20	-11 ≤ <i>h</i> ≤ 11, -11 ≤ <i>k</i> ≤ 10, -15 ≤ <i>l</i> ≤ 14
Reflections collected	17810	37714	8950
Independent reflections	4109 [<i>R</i> (int) = 0.0471]	4669 [<i>R</i> (int) = 0.0360]	4156 [<i>R</i> (int) = 0.0446]
Completeness to θ = 27.48	96.1 %	99.9 %	98.7 %
Absorption correction	Semi-empirical from equivalents	Semi-empirical from equivalents	Semi-empirical from equivalents
Max. and min. transmission	0.987 and 0.982	0.987 and 0.983	0.9868 and 0.9829
Refinement method	Full-matrix least-squares on <i>F</i> ²	Full-matrix least-squares on <i>F</i> ²	Full-matrix least-squares on <i>F</i> ²
Data / restraints / parameters	4109 / 6 / 352	4669 / 0 / 327	4156 / 72 / 327
Goodness-of-fit on <i>F</i> ²	1.083	1.047	0.980
Final <i>R</i> indices [<i>I</i> > 2 σ (<i>I</i>)]	<i>R</i> ₁ = 0.0860, w <i>R</i> ₂ = 0.2328	<i>R</i> ₁ = 0.0616, w <i>R</i> ₂ = 0.1597	<i>R</i> ₁ = 0.0624, w <i>R</i> ₂ = 0.1827
<i>R</i> indices (all data)	<i>R</i> ₁ = 0.1263, w <i>R</i> ₂ = 0.2626	<i>R</i> ₁ = 0.0805, w <i>R</i> ₂ = 0.1751	<i>R</i> ₁ = 0.1119, w <i>R</i> ₂ = 0.2277
Largest diff. peak and hole/e Å ⁻³	0.330 and -0.211	0.267 and -0.197	0.412 and -0.327
CCDC	1863051	1863052	1863053

3. Photodimerization reaction

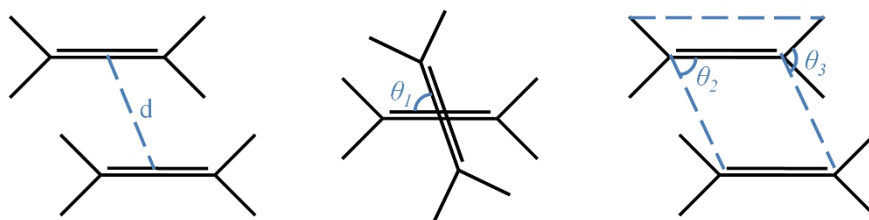


Fig. S12 The parameters are usually considered to be geometric criteria for [2+2] cycloaddition.

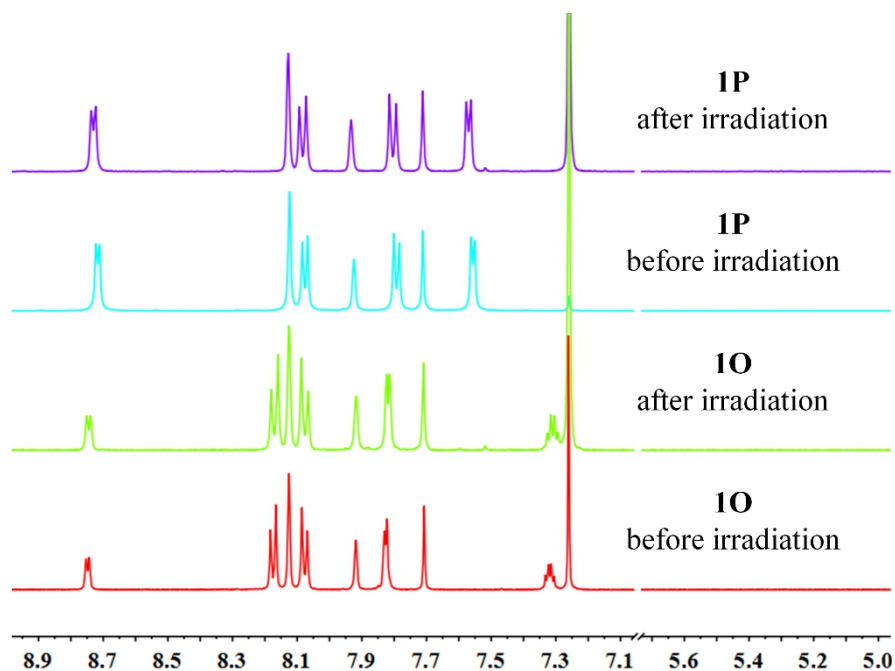


Fig. S13 $^1\text{H-NMR}$ spectra of 1O and 1P crystals (14 mM) before and after irradiation.

Synthesis of photodimerization product *c*-1M

The powder of 1M (0.30 g, 0.72 mmol) in the nuclear magnetic tubes was irradiated with 365 nm UV light from a 20 W LED lamp for 30 min. The crude product was purified by silica-gel chromatography using ethyl acetate/ CH_2Cl_2 mixture (1:10, v/v) as eluent to obtain *c*-1M (0.20 g, yield 67%).

$^1\text{H-NMR}$ (500 MHz, CDCl_3) δ/ppm = 8.80 (s, 2H), 8.64 (d, J = 3.9 Hz, 2H), 7.85 (s, 2H), 7.82 (d, J = 7.9 Hz, 2H), 7.71 (s, 4H), 7.59 (d, J = 8.1 Hz, 4H), 7.45 (d, J = 8.1 Hz, 4H), 7.39 (dd, J = 7.6, 4.9 Hz, 2H), 5.39 (s, 2H). $^{13}\text{C-NMR}$ (126 MHz, CDCl_3) δ/ppm = 149.43, 148.33, 140.07, 136.94, 135.23, 134.52, 132.73 (q, J = 34.17 Hz), 130.76, 130.23, 128.37, 128.26, 123.83, 123.26, 122.63 (q, J = 273.83 Hz), 119.91, 55.64 and 47.34.

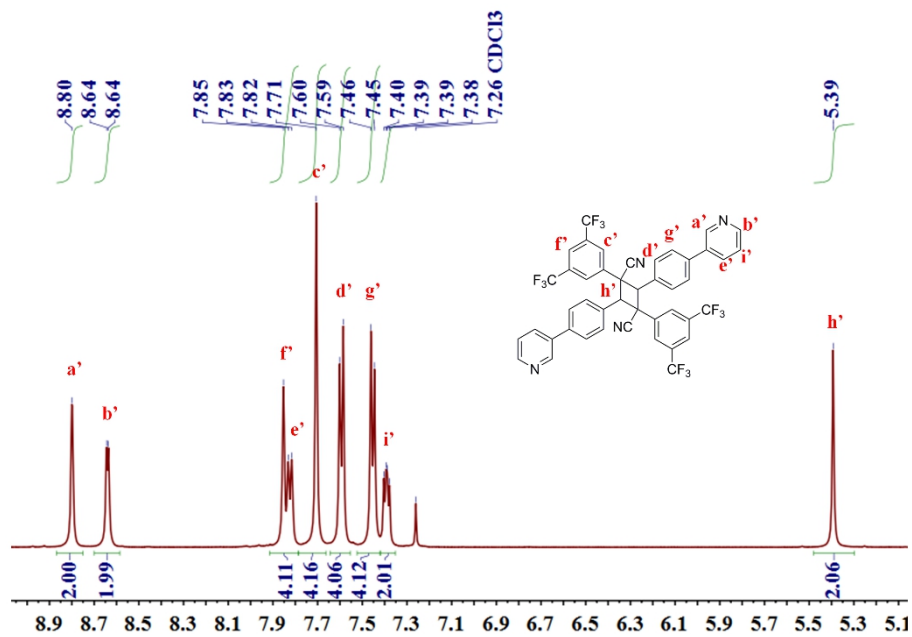


Fig. S14 ¹H-NMR spectrum of *c*-1M (98 mM) in CDCl₃.

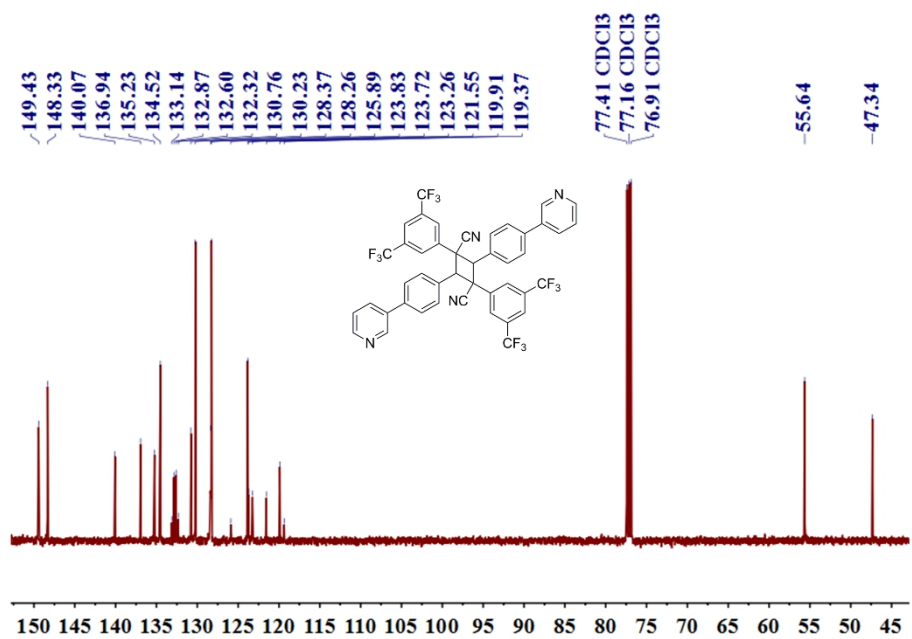


Fig. S15 ¹³C-NMR spectrum of *c*-1M (98 mM) in CDCl₃.

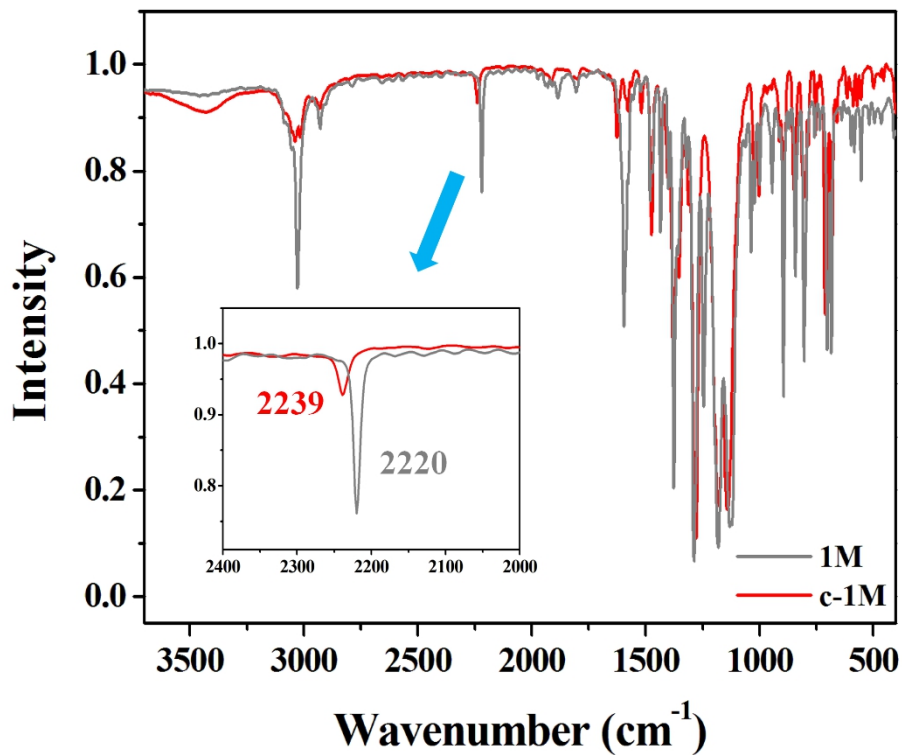


Fig. S16 FT-IR spectra of 1M and *c*-1M. Insert: amplifying curves of cyano stretching peaks.

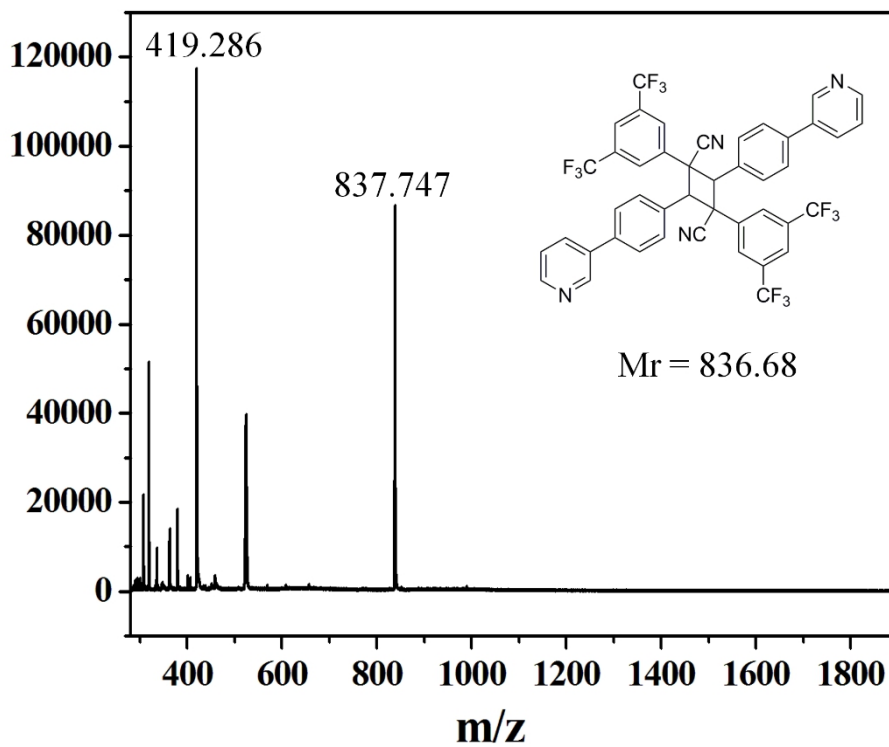


Fig. S17 MALDI-TOF mass spectrum of *c*-1M.

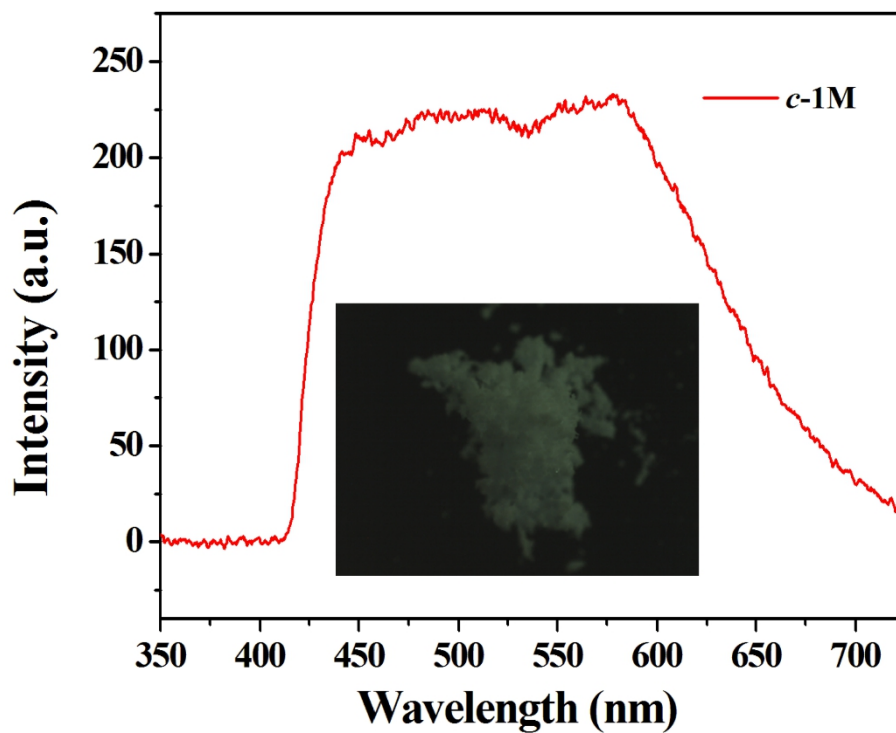


Fig. S18 PL spectrum of *c*-1M powder and inset is fluorescence microscopy image of pure *c*-1M ($\lambda_{\text{ex}} = 365$ nm).

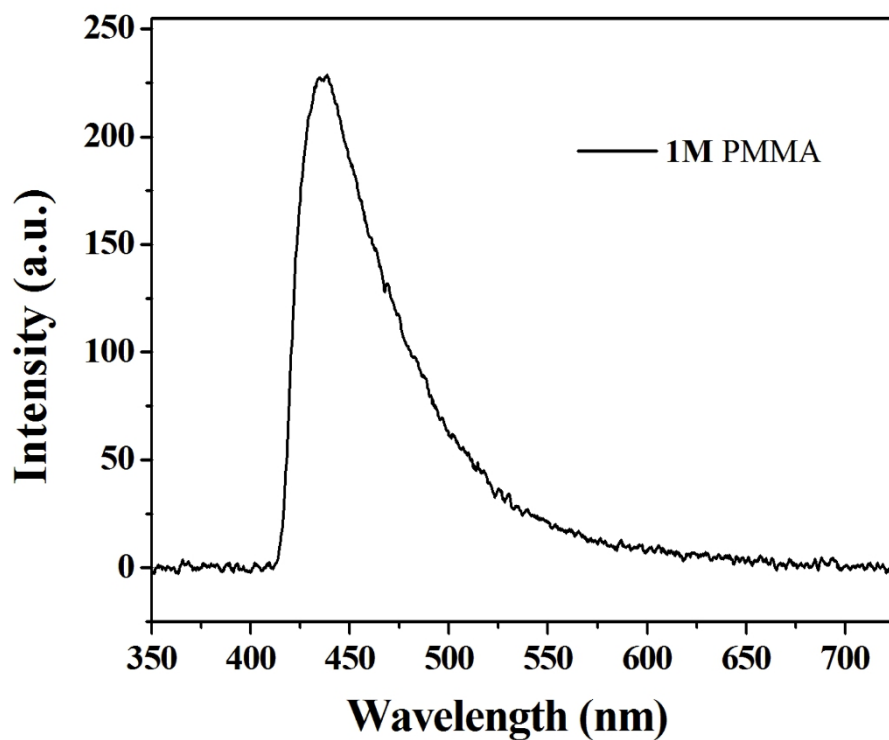


Fig. S19 PL spectrum ($\lambda_{\text{ex}} = 365$ nm) of 1M of 3% wt. in polymethylmethacrylate (PMMA).

4. Characterization of cocrystals

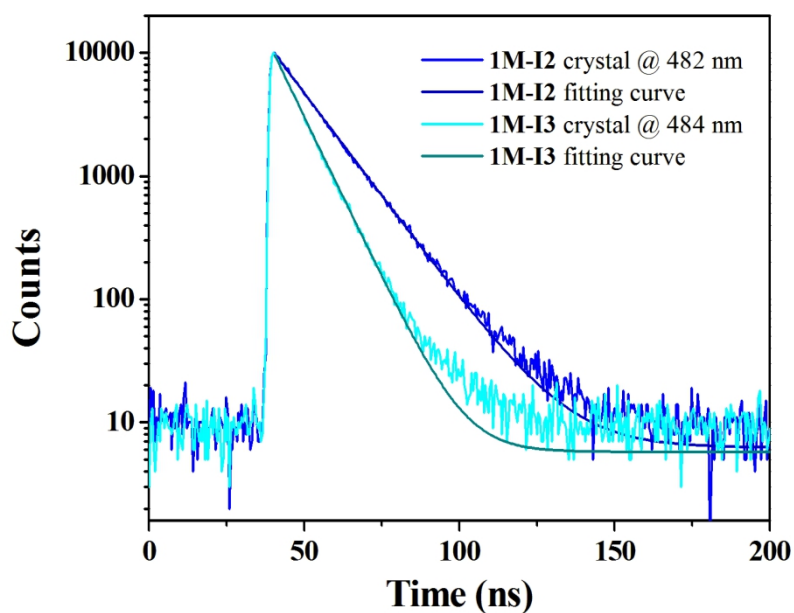


Fig. S20 The lifetimes of 1M-I2 and 1M-I3 in the crystal states ($\lambda_{\text{ex}} = 365 \text{ nm}$).

Table S3 The photophysical properties of cocrystals 1M-I2 and 1M-I3

Compound	PL (nm)	τ (ns)	PLQY	k_r (s^{-1}) ^a	k_{nr} (s^{-1}) ^b
1M-I2	482	12.98	0.55	4.230×10^7	3.475×10^7
1M-I3	484	8.29	0.41	4.989×10^7	7.079×10^7

^aRadiative transition rate constant: $k_r = \Phi_F / \langle \tau \rangle$.

^bNon-radiative transition rate constant: $k_{\text{nr}} = (1 - \Phi_F) / \langle \tau \rangle$. $\langle \tau \rangle = (A_1 \tau_1^2 + A_2 \tau_2^2) / (A_1 \tau_1 + A_2 \tau_2)$.

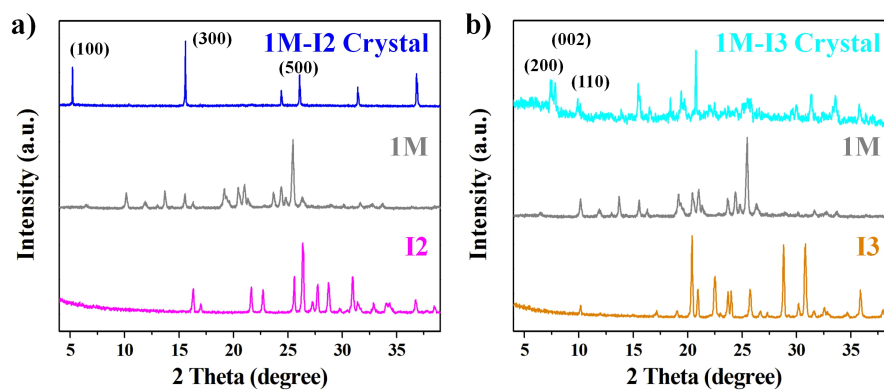


Fig. S21 XRD patterns of the cocrystals (a) 1M-I2, (b) 1M-I3 and their components.

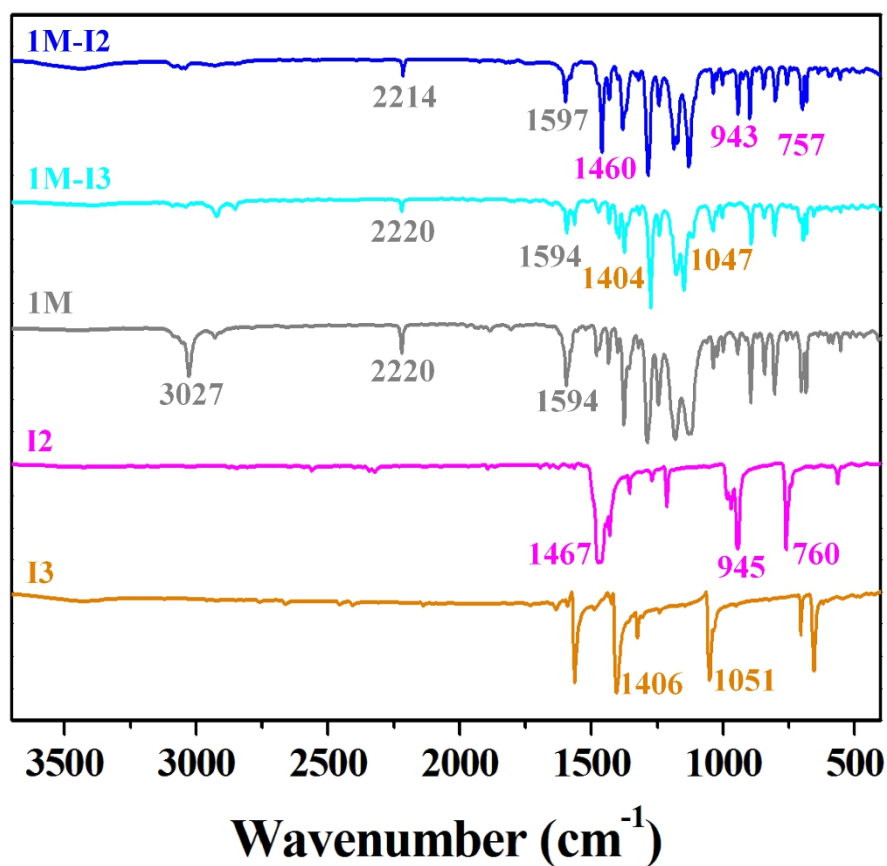


Fig. S22 FT-IR spectra of molecules I2, I3, 1M, 1M-I2 and 1M-I3.

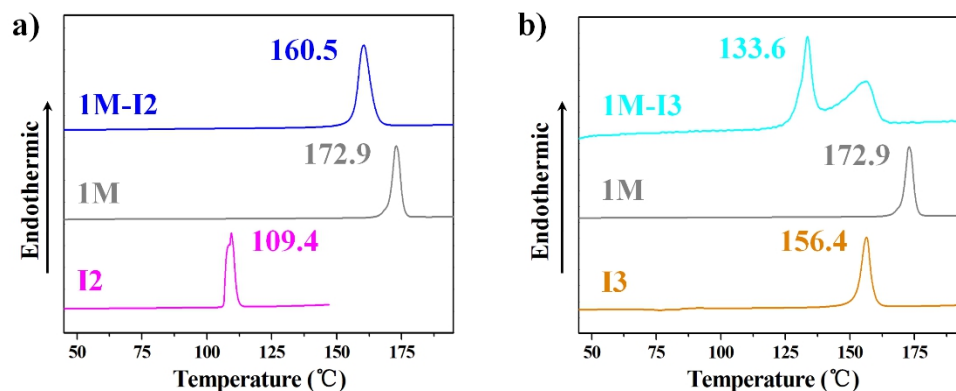


Fig. S23 Thermal analysis of the complexes (a) 1M-I2, (b) 1M-I3 and their components (20 °C min^{-1} on the second heating cycle).

Table S4 Crystal data and structure refinements for 1M-I2 and 1M-I3

Compound	1M-I2	1M-I3
Empirical formula	C ₅₀ H ₂₄ F ₁₆ I ₂ N ₄	C ₅₀ H ₂₄ F ₁₅ I ₃ N ₄
Formula weight/g mol ⁻¹	1238.53	1346.43
<i>T</i> /K	293(2)	293(2)
λ /Å	0.71073	0.71073
Crystal system	Monoclinic	Monoclinic
Space group	<i>P</i> 2 ₁ / <i>c</i>	<i>C</i> 2/ <i>c</i>
Unit cell dimensions/Å	<i>a</i> = 17.0950(5) <i>b</i> = 14.8620(4) <i>c</i> = 9.2252(3)	<i>a</i> = 24.2597(17) <i>b</i> = 9.1991(5) <i>c</i> = 23.5097(13)
Unit cell angles/°	α = 90 β = 91.4590(10) γ = 90	α = 90 β = 103.794(4) γ = 90
Volume/Å ³	2343.05(12)	5095.3(5)
<i>Z</i>	2	4
ρ (calculated)/Mg m ⁻³	1.756	1.755
Absorption coefficient/mm ⁻¹	1.447	1.934
<i>F</i> (000)	1204	2584
Crystal size/mm ³	0.130 × 0.120 × 0.100	0.130 × 0.120 × 0.100
θ range for data collection/°	2.750 to 28.275	2.765 to 27.477
Index ranges	-22 ≤ <i>h</i> ≤ 22, -19 ≤ <i>k</i> ≤ 19, -12 ≤ <i>l</i> ≤ 11	-31 ≤ <i>h</i> ≤ 31, -11 ≤ <i>k</i> ≤ 11, -30 ≤ <i>l</i> ≤ 30
Reflections collected	27896	52240
Independent reflections	5804 [<i>R</i> (int) = 0.0230]	5814 [<i>R</i> (int) = 0.0404]
Completeness to θ = 27.48	99.8 %	99.8 %
Absorption correction	Semi-empirical from equivalents	Semi-empirical from equivalents
Max. and min. transmission	0.869 and 0.834	0.830 and 0.787
Refinement method	Full-matrix least-squares on <i>F</i> ²	Full-matrix least-squares on <i>F</i> ²
Data / restraints / parameters	5804 / 0 / 433	5814 / 12 / 381
Goodness-of-fit on <i>F</i> ²	1.025	1.066
Final <i>R</i> indices [<i>I</i> > 2 σ (<i>I</i>)]	<i>R</i> ₁ = 0.0360, w <i>R</i> ₂ = 0.0901	<i>R</i> ₁ = 0.0474, w <i>R</i> ₂ = 0.1094
<i>R</i> indices (all data)	<i>R</i> ₁ = 0.0499, w <i>R</i> ₂ = 0.1001	<i>R</i> ₁ = 0.0643, w <i>R</i> ₂ = 0.1245
Large st diff. peak and hole/e Å ⁻³	0.472 and -0.660	1.509 and -1.147
CCDC	1863054	1863055

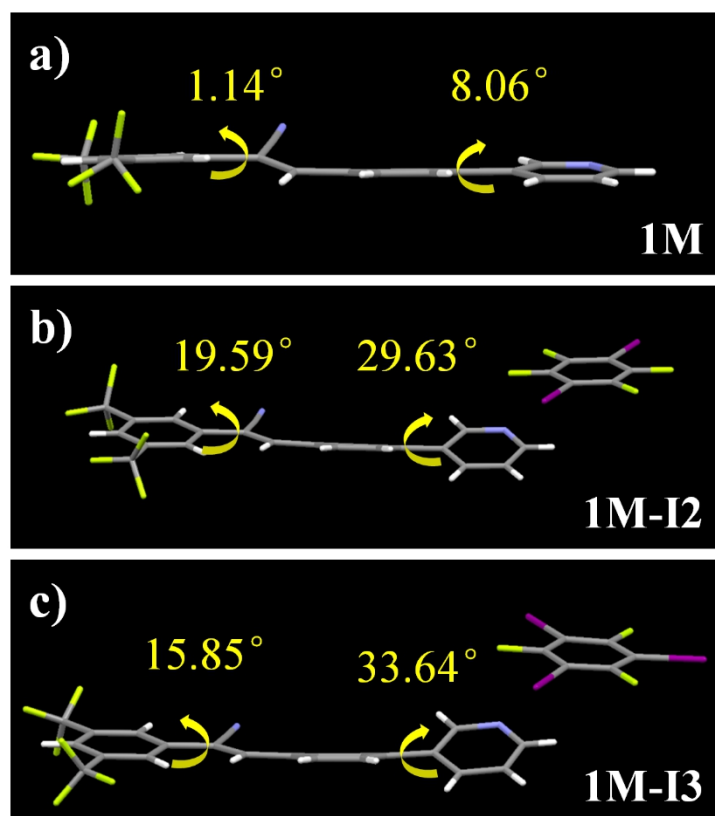


Fig. S24 Molecular configurations in the crystals of (a) 1M, (b) 1M-I2 and (c) 1M-I3.

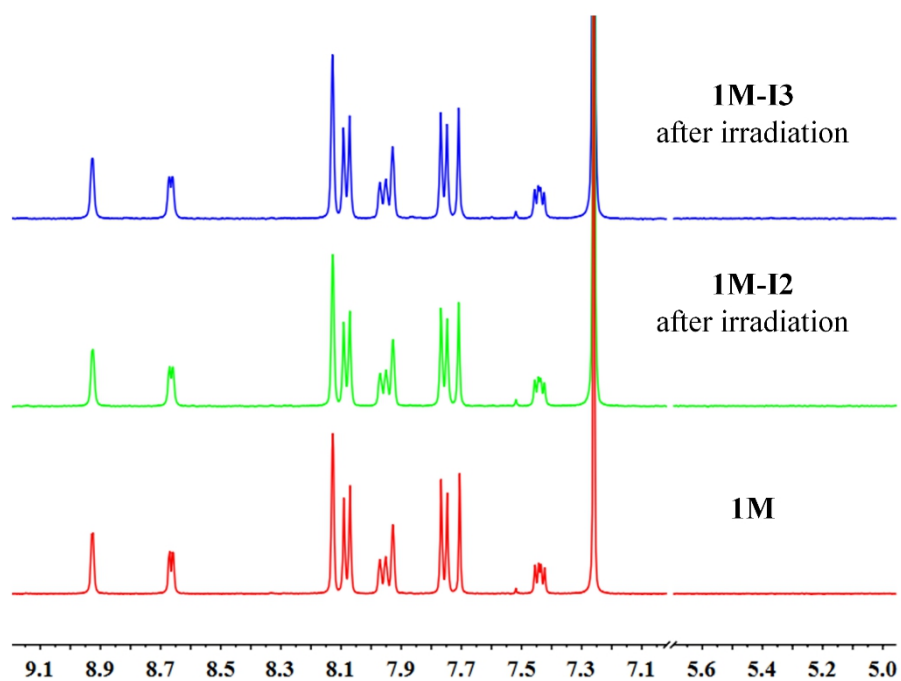


Fig. S25 $^1\text{H-NMR}$ spectra of 1M, 1M-I2 and 1M-I3 (14 mM) after irradiation.

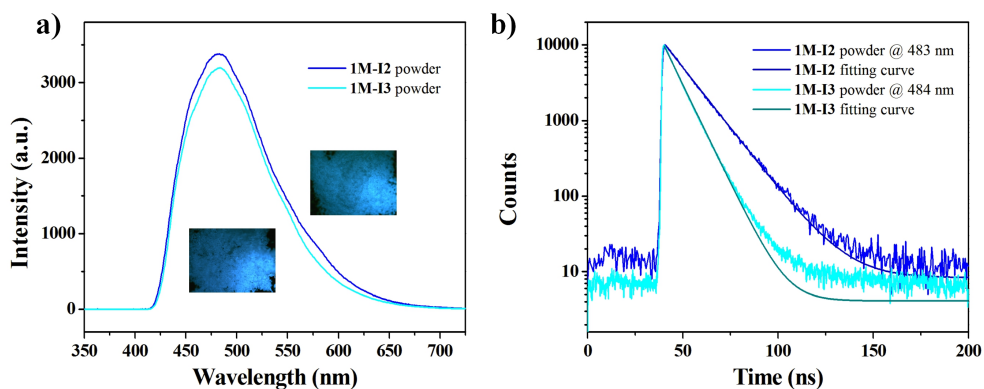


Fig. S26 PL spectra and lifetimes of powders for (a) 1M-I2 and (b) 1M-I3. The insets show the fluorescent microphotographs of powders, respectively ($\lambda_{\text{ex}} = 365$ nm).

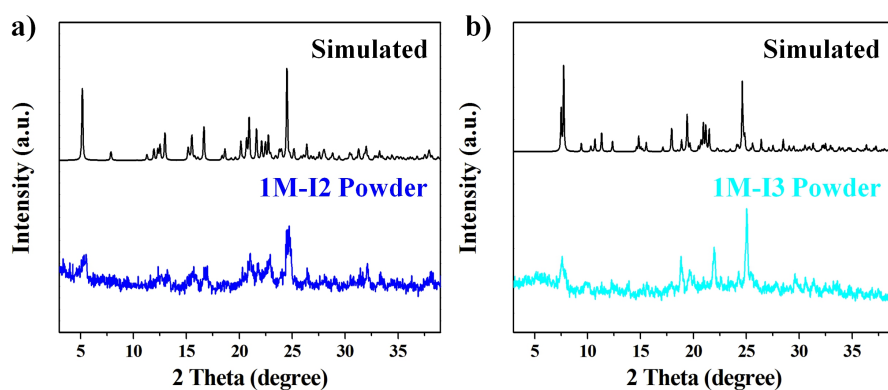


Fig. S27 Experimental XRD patterns of (a) 1M-I2 powder and (b) 1M-I3 powder and the calculated diffraction patterns based on the single crystal data.

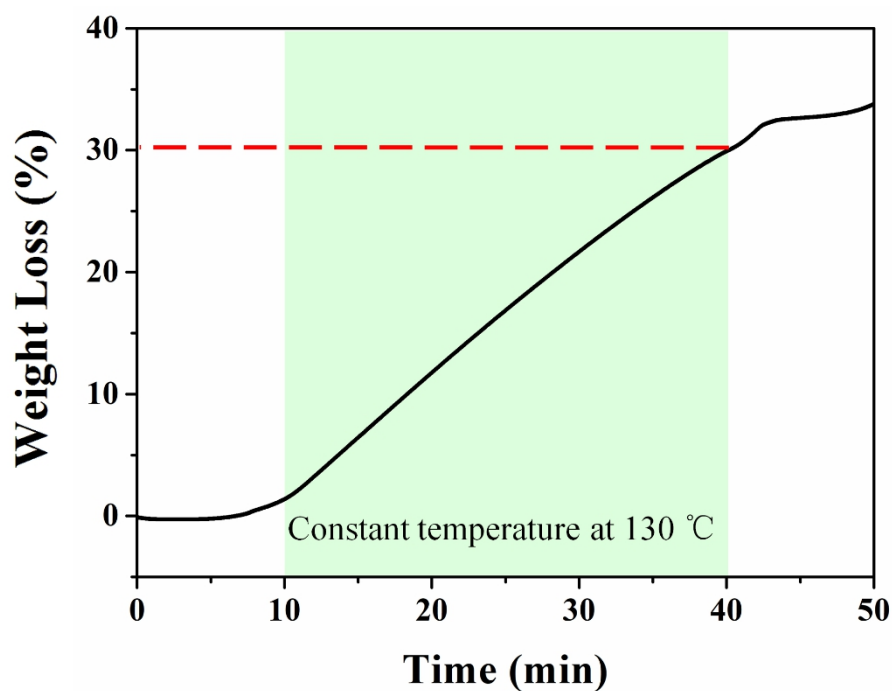


Fig. S28 Constant temperature weight loss curve of 1M-I2.

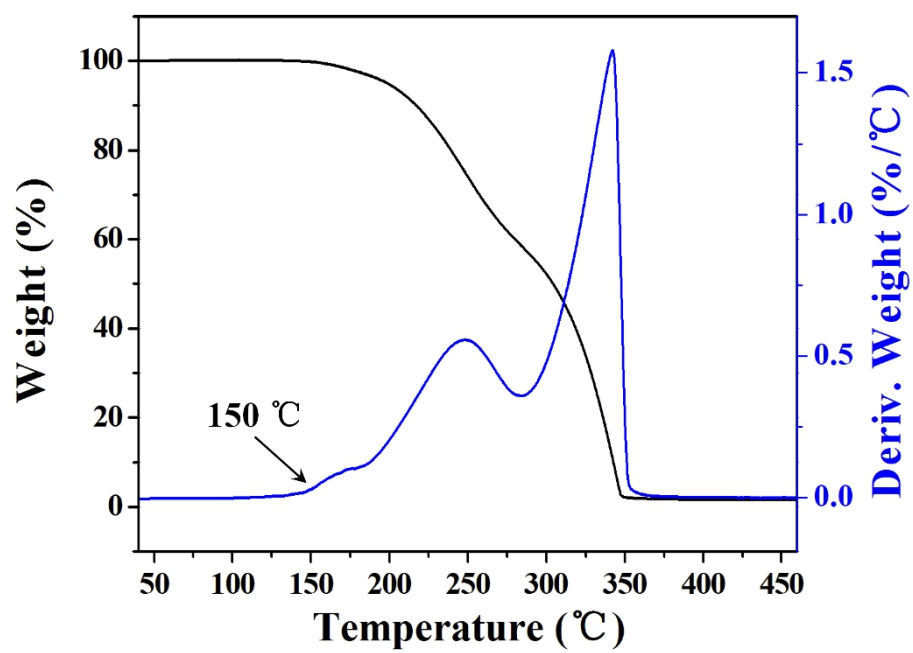


Fig. S29 TGA curve of cocrystal 1M-I3 (10 °C min⁻¹).